Lloyd & Heathcote 1985

Lloyd, J. W. & Heathcote, J. A. (1985): The representation of hydrochemical data as a basis for interpretation. – Natural inorganic chemistry in relation to groundwater – An introduction. – p. 113-142, 28 Abb.; Oxford (Clarendon).

6 The representation of hydrochemical data as a basis for interpretation

6.1. Introduction

As can be seen from the discussions in the previous chapters, well-head measurements, laboratory analyses, and calculations provide a plethora of hydrochemical parameters on which interpretation can be based. The multitude of chemical data frequently amassed in groundwater studies can, however, pose problems, as without a methodical approach to the analysis of the data the hydrochemical processes occurring, the influence of hydrogeological controls, etc. can be confused and the data may appear contradictory.

In this chapter the representation of hydrochemical data is discussed with respect to understanding hydrochemical distributions, the basis for assessing the relationship between differing hydrochemical water types, and some of the processes involved in the chemical evolution of groundwaters.

It is stressed that although a sensible general approach to the analysis of data can be adopted and normally general hydrochemical processes can be recognized in any hydrogeological situation, each situation should be considered as being unique so that only some of the techniques described below will be applicable in each individual study, and applicability may vary from study to study.

In the procedure of representing data for interpretation it is recommended that a twofold approach be adopted which should consist firstly of maps of distribution of pertinent parameters and secondly of relevant parameter relationship diagrams. It is emphasized that the two types of representation should be used concurrently. Further, while representation is essential for interpretation it is also important for displaying data coherently and for communicating the complexity of interpretation.

6.2. Distribution maps

The most frequently used distribution maps are those depicting total dissolved solids or electrical conductivity. Such maps provide useful preliminary information about a system together with water quality indications.

In Fig. 6.1 a total dissolved solids distribution is compared with a groundwater flow net for the Lower Palaeozoic Disi Sandstone aquifer in Southern Jordan. The groundwater flow in the area is partly influenced by a vertical dyke and the control is reflected by the hydrochemistry. Similarly, the geological structure in the Lincolnshire Limestone (Fig. 6.2) is believed to control the

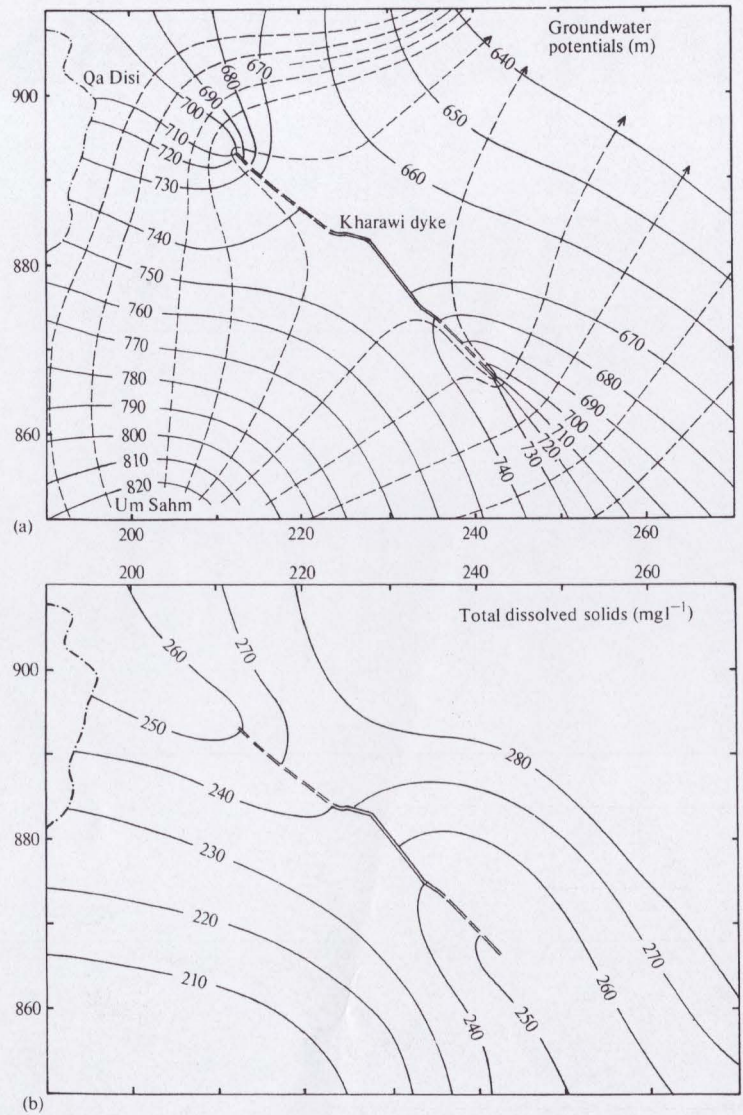

Fig. 6.1. Relationship between a flow net (map (a)) and total dissolved solids distribution (map (b)) for the southern desert of Jordan. (After Lloyd 1969.)

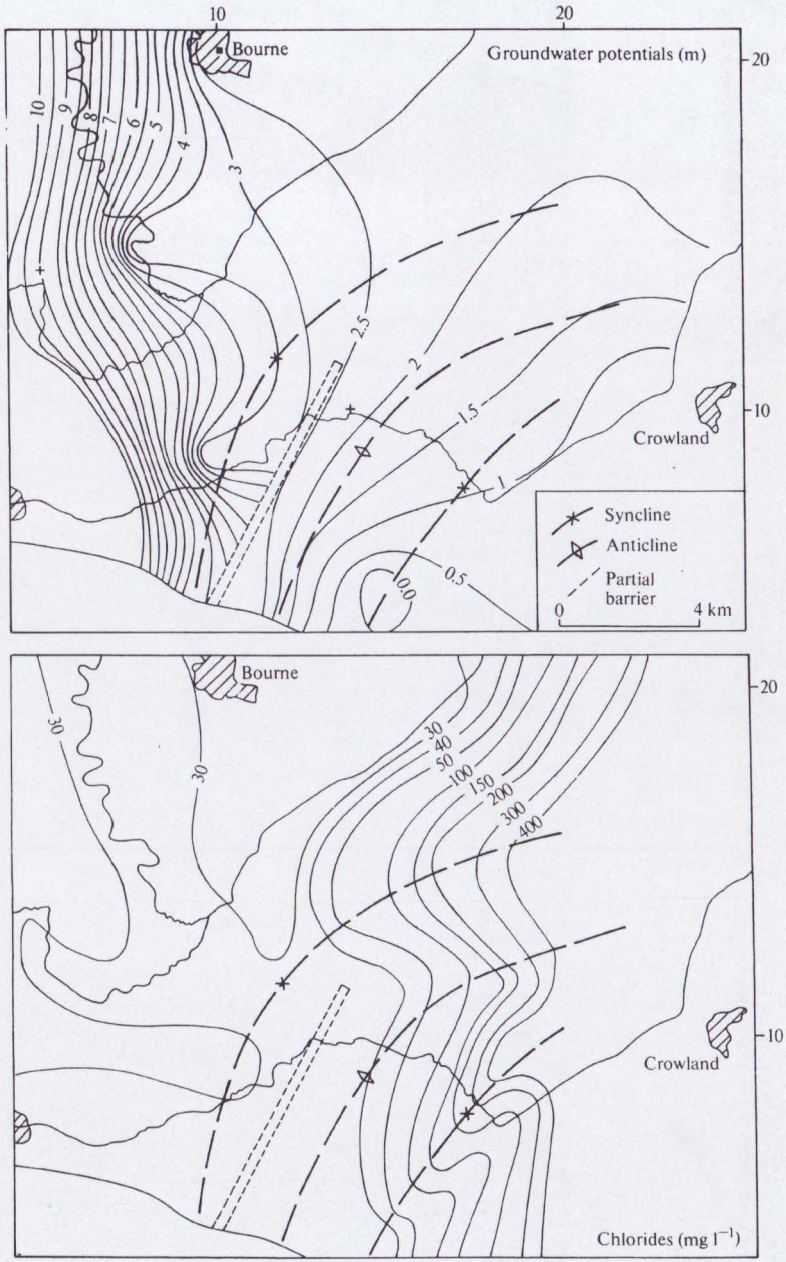

Fig. 6.2. Groundwater potential distribution for part of the Lincolnshire Limestone aquifer and chloride distribution showing influences of geological structural control.

hydrochemistry (Marsh 1977). Flow is shown conforming to a partial barrier boundary attributed to a low permeability zone on an anticlinal flank with chloride concentrations reflecting the boundary in a subdued manner. Low flow conditions along the eastern syncline are clearly reflected by the chlorides. Total dissolved solids maps, however, have limitations in that they are bulk parameters and not unique. For distribution maps it is therefore preferable to use individual ions, ion ratios, or certain calculated parameters.

In hydrochemical groundwater evolution the chloride ion tends to be the most conservative in that it is readily removed from matrix materials but rarely precipitated under dilute solution conditions. Chloride concentrations therefore normally increase down the hydraulic gradient and with groundwater flow experience and residence. The normal chloride concentration increase is only disturbed where pollution or dilution occurs so that chloride is an excellent indicator of groundwater flow direction and preferential permeability conditions.

In constructing distribution maps it is essential that they relate to the hydrogeological controls and reflect the piezometry of the aquifer system. One of the main values of distribution maps is that they provide an independent check on piezometry and can reveal hydrogeological conditions which are not necessarily apparent from the piezometry. This is particularly so where piezometry is highly disturbed by abstraction.

Maps of hydrochemical ratios have long been favoured by French workers and can provide useful information concerning such features as ion exchange and the onset of brackish water influences. An example of ratio maps and the associated total dissolved solids is given in Fig. 6.3 for the Mornag alluvial aquifer in Tunisia.

6.3. Hydrochemical sections

While distribution maps indicate rates of change of chemical concentration regionally and can be thus interpreted, the overall trends are probably better represented and understood using hydrochemical sections on which a number of parameters can be shown. Such diagrams depict associated changes in parameter values and aid in interpreting the controlling hydrochemical processes.

Hydrochemical sections can be constructed along specific groundwater flow lines, but normally are constructed in the direction of declining hydraulic head from either a recharge mound or the start of a confining cover using an associated set of regional data. Where complex groundwater flow occurs total dissolved solids can be used as the abscissa.

On Fig. 6.4 a confined aquifer hydrochemical section is shown for the Lincolnshire Limestone in which a classical redox barrier with the associated hydrochemical changes along the hydraulic groundwater gradient are depicted. Changes in alkalinity and the various hardness parameters can also be depicted

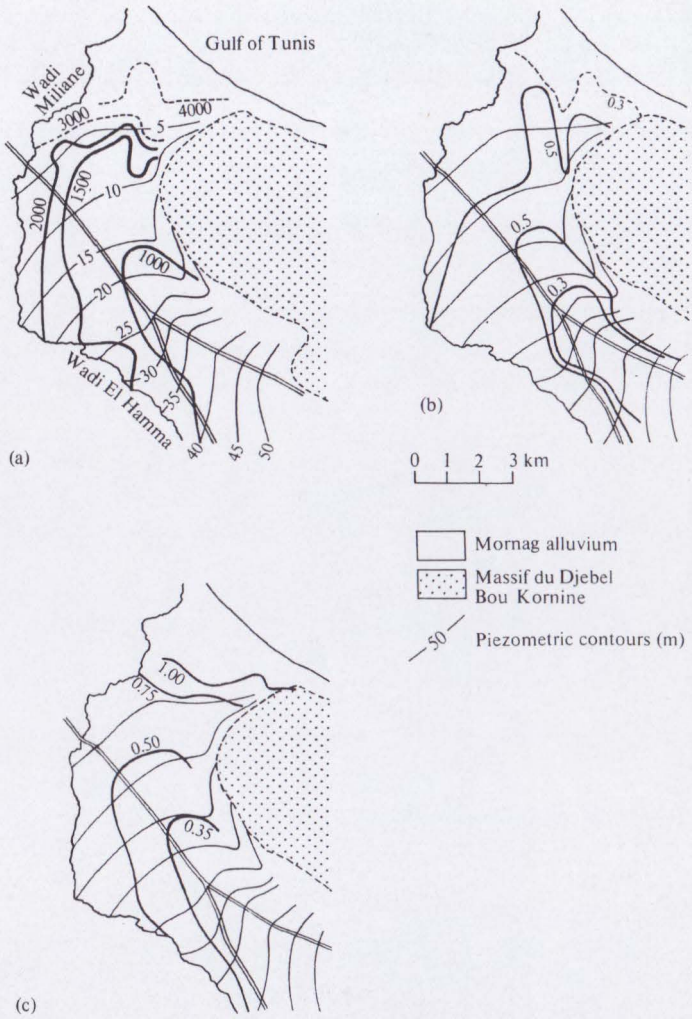

Fig. 6.3. Hydrochemical ratio distributions from the Mornag alluvium aquifer, Tunisia: (a) map of total dissolved solids (mg l^{-1}); (b) map of SO_4^{2-}/Cl^- ratios; (c) map of Mg^{2+}/Ca^{2+} ratios. N.B. Location and piezometric contours are shown in all three maps. (After Schoeller 1959.)

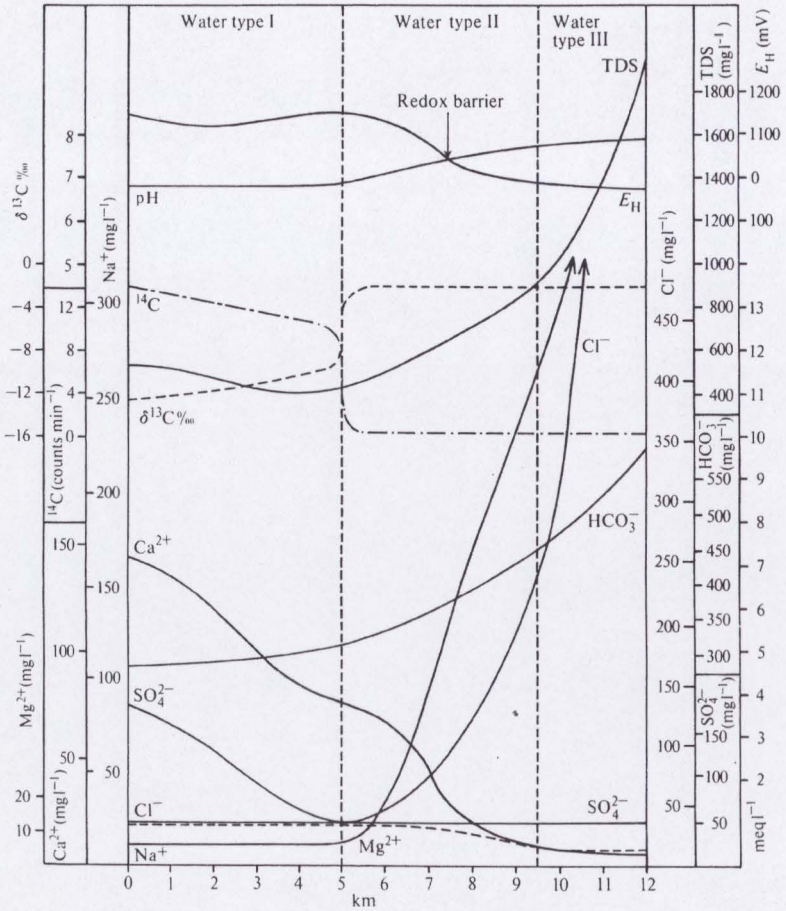

Fig. 6.4. Hydrochemical section for part of the central Lincolnshire Limestone. (After Lawrence, Lloyd, and Marsh 1976.)

to advantage by hydrochemical sections as shown in Fig. 6.5 for part of the London Basin chalk aquifer.

6.4. Hydrochemical diagrams

Graphical representations of hydrochemical data pose considerable problems. Dimension limitations severely restrict illustration to all but the most simple forms, while graphical representation of statistically derived hydrochemical functions, although attractive, is frequently difficult to comprehend. Hydrochemical diagrams need to be as comprehensive as possible and in addition

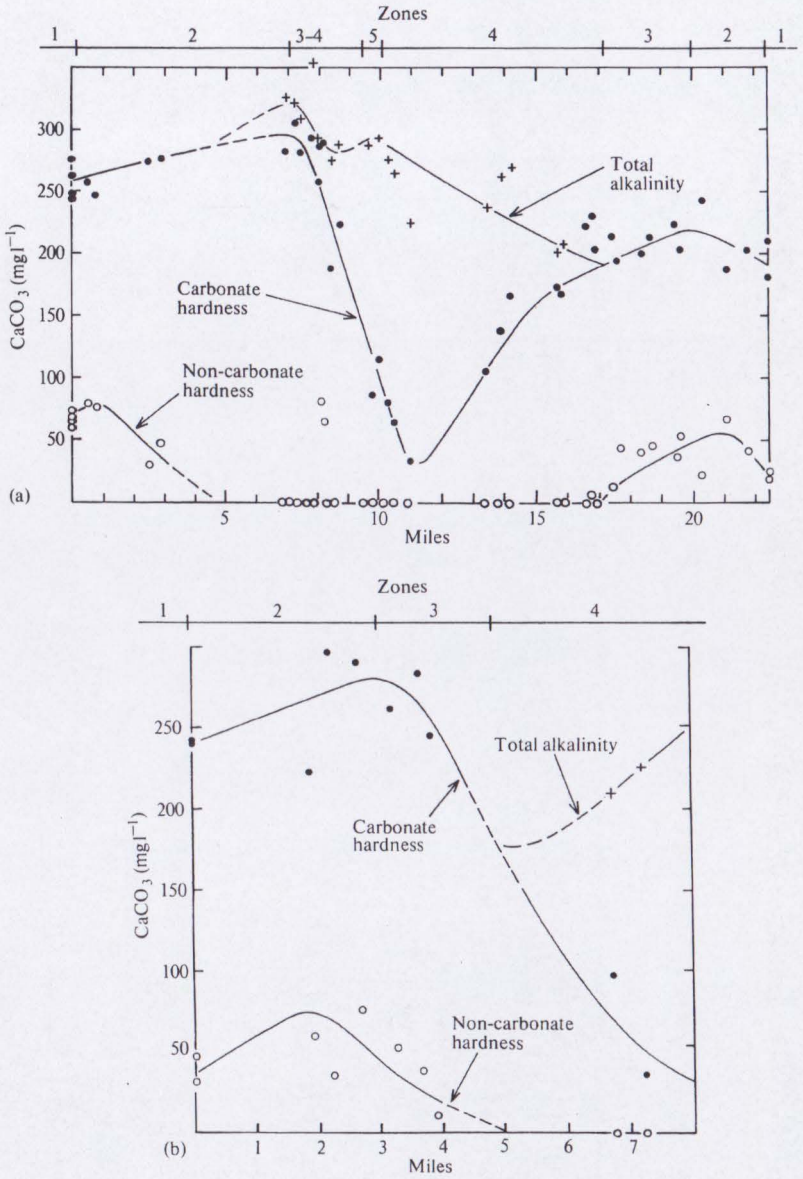

Fig. 6.5. Hydrochemical sections of alkalinity and hardness in the chalk of (a) the London Basin and (b) North Kent: +, total alkalinity; •, carbonate hardness; ○, non-carbonate hardness. (After Ineson and Dowing 1963.)

should facilitate interpretation of evolutionary trends and hydrochemical processes. Few diagrams really possess these features. In using hydrochemical diagrams it is re-emphasized that their real value is realized when they are interpreted in conjunction with distribution maps.

6.4.1. Vertical bar graphs

A vertical bar graph of groundwater analyses is shown in Fig. 6.6(a). Each analysis appears as a vertical bar with a height proportional to the total concentration of anions or cations, normally expressed in milliequivalents per litre. Individual ion concentrations are depicted proportionally in a consistent pattern. While the major ions are shown on Fig. 6.6, clearly any parameter permutation can be used. As shown in Fig. 6.6(b) an analysis can be demonstrated in terms of the percentage of total milliequivalents per litre.

6.4.2. Vector diagrams

A vector diagram representing major ion chemistry for several groundwater analyses is shown in Fig. 6.7. The lengths of the six vectors represent ionic concentrations in milliequivalents per litre. Such diagrams appear to have little merit.

6.4.3. Circular and radial diagrams

Circular diagrams of hydrochemical analyses (Fig. 6.8) are constructed with their radii proportional to the total ionic concentrations. Sectors within a circle represent fractions of the different ions expressed as milliequivalents per litre. A radial diagram is shown in Fig. 6.9. On the diagram the ions are scaled and the intercepts are joined to represent the water. As with vector diagrams only one analysis is represented on circular and radial diagrams so they are of limited value.

6.4.4. Pattern diagrams

Pattern diagrams were first devised by Stiff (1951) to represent analyses in distinctive graphical shapes by plotting ions in milliequivalents per litre on on parallel axes as illustrated in Fig. 6.10. While pattern diagrams can show differences between individual chemical analyses, they suffer from the same limitations as discussed for the previous diagrams.

6.4.5. Semilogarithmic diagrams

Semilogarithmic diagrams were developed by Schoeller (1962) to represent major ion analyses in milliequivalents per litre and to demonstrate different hydrochemical water types on the same diagram. A semilogarithmic diagram is shown in Fig. 6.11 with two water types clearly depicted. Because of the line work, unfortunately only a few analyses can usually be illustrated. The diagram has one advantage over the more universally used trilinear diagrams discussed below in that actual parameter concentrations are given. The diagrams can be

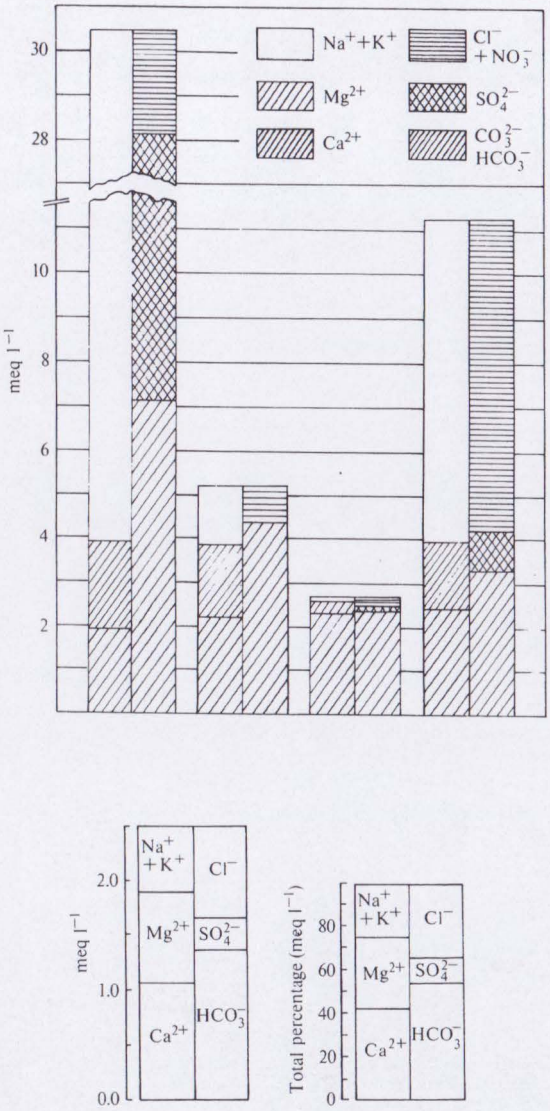

Fig. 6.6. Major ion chemistry represented by bar charts.

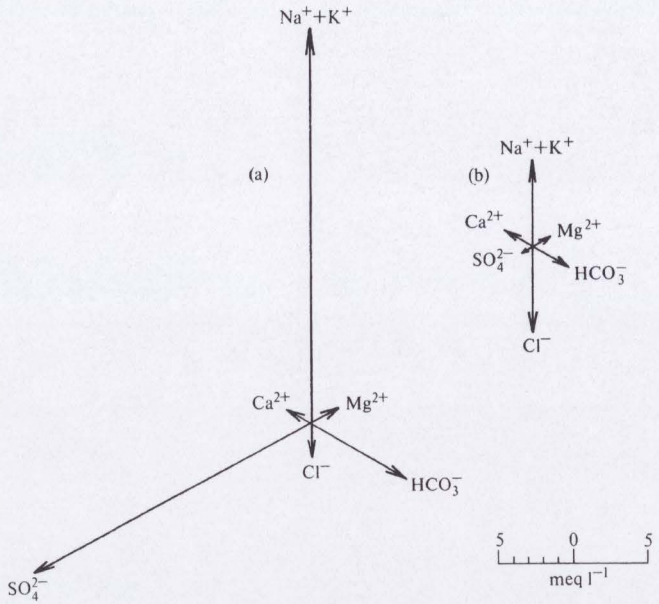

	(a)		(b)	
	mg l^{-1}	meq l^{-1}	mg l^{-1}	meq l^{-1}
Ca^{2+}	37	1.85	49	2.45
Mg^{2+}	24	1.97	18	1.48
$Na^{+}+K^{+}$	611	26.58	168	7.29
HCO_3^-	429	7.03	202	3.31
SO_4^{2-}	1010	21.03	44	0.92
Cl^-	82	2.31	246	6.94

Fig. 6.7. Vector diagram for major ions. (After Maucha 1949.)

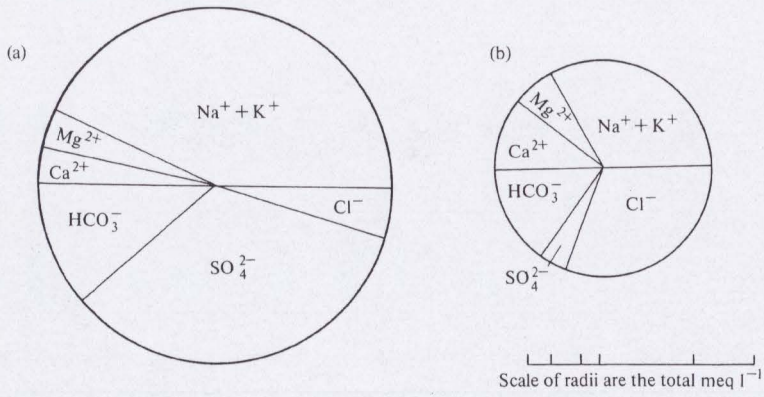

Fig. 6.8. Circular diagram for major ions (analyses shown on Fig. 6.7). (After Hem 1970.)

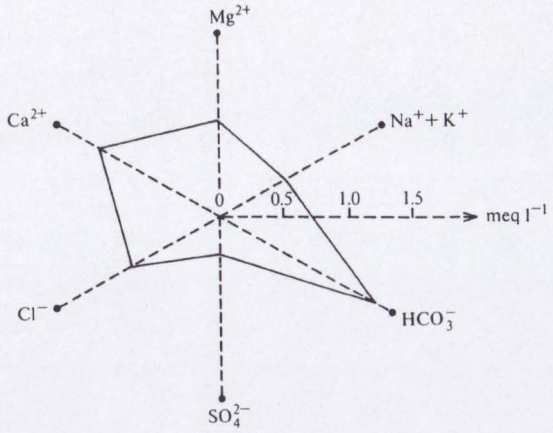

	mg l^{-1}	meq l^{-1}
Ca^{2+}	21	1.05
Mg^{2+}	9	0.73
$Na^{+}+K^{+}$	14	0.58
HCO_3^{-}	84	1.38
SO_4^{2-}	13	0.27
Cl^{-}	27	0.76

Fig. 6.9. Radial diagram for major ions.

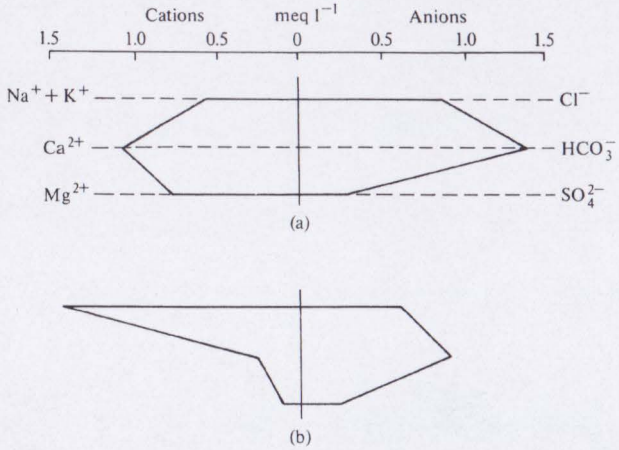

	(a)		(b)	
	mg l^{-1}	meq l^{-1}	mg l^{-1}	meq l^{-1}
Ca^{2+}	22	1.10	5	0.25
Mg^{2+}	9.4	0.77	1.4	0.12
$Na^{+}+K^{+}$	13	0.55	35	1.45
HCO_3^{-}	84	1.38	55	0.90
SO_4^{2-}	12	0.25	11	0.23
Cl^{-}	31	0.87	21	0.59

Fig. 6.10. Pattern diagram for major ions. (After Stiff 1951.)

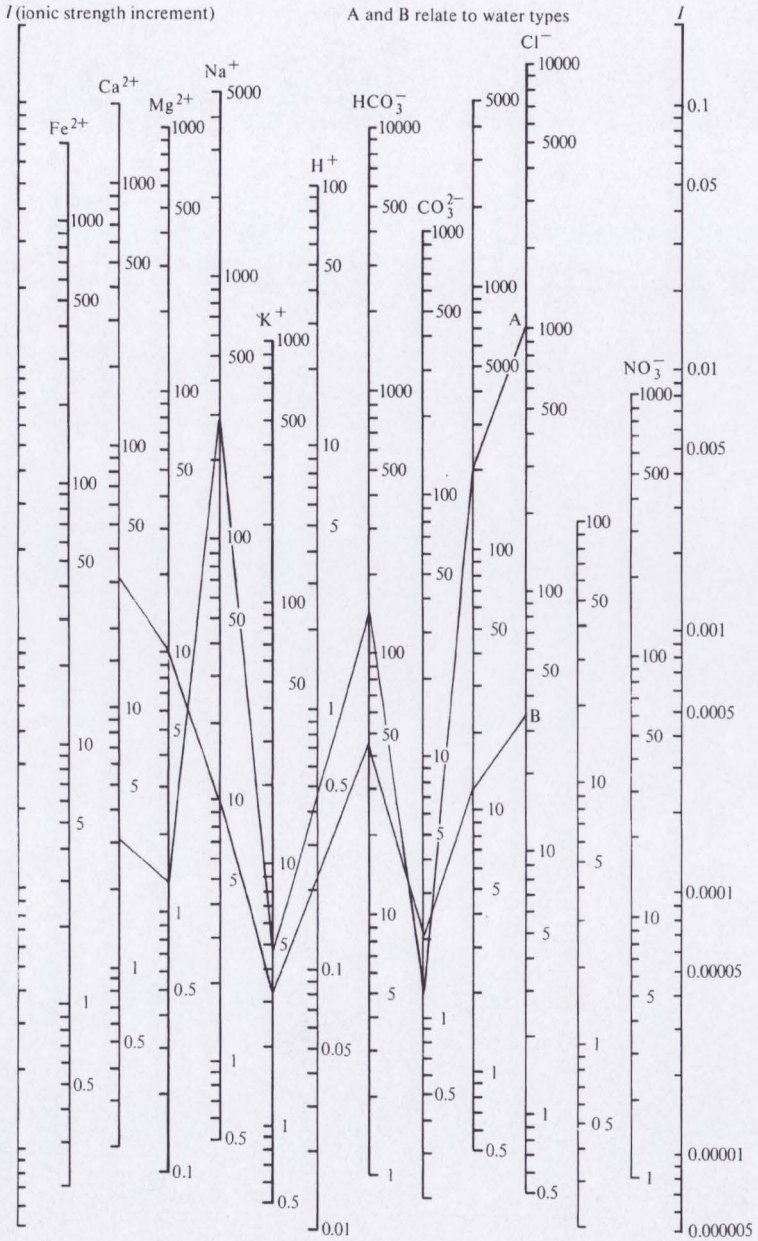

Fig. 6.11. Semilogarithmic diagram for major ions (mg l^{-1}). (After Schoeller 1962.)

adapted to determine the degree of calcite saturation as demonstrated by Schoeller (1962), although this has little advantage today in view of computational facilities.

Semilogarithmic diagrams can be used in a simplified form to represent any parameters, for example a heavy metal suite.

6.4.6. X-Y plots

X-Y plots are the most simple and obvious initial approach to the interpretation of hydrochemical data. With modern computer graphical facilities such plots can rapidly be compiled for a large number of *X-Y* relationships which will allow a preliminary assessment of those parameters that may assist in interpretation. Plots of single ion relationships and those ion ratios that may prove meaningful can easily be established. Ratios considered include Ca^{2+}: Mg^{2+}, Ca^{2+}: Na^{+}, Na^{+}: $Ca^{2+} + Mg^{2+}$, HCO_3^-: Cl^-, SO_4^{2-}: Cl^-, Cl^-–Na^+: Cl^-, etc.

For ion *X-Y* plots the stoichiometric balance between ions, if pertinent, can be represented for pairs of ions to examine possible process effects. For example the stoichiometry shown on Fig. 6.12 for $Ca^{2+}/(HCO_3^- + SO_4^{2-})$ and Na^+/Cl^- indicates a ratio close to 1.0, showing that for the particular groundwaters being studied neither ion exchange nor sulphate reduction, for example, are complicating the carbonate chemistry and simple solution is the main process.

6.4.7. Dilution diagrams

A variation of the *X-Y* plot is the dilution diagram in which the groundwaters in a system are compared with respect to two end-point waters. Such diagrams are usually plotted semilogarithmically or logarithmically. The dilution line represents a percentage mixing between the two end-point waters so that waters plotting away from the line indicate preferential enrichment or depletion by one ion with respect to the other which may infer a certain chemical process control.

A dilution diagram for a set of saline groundwaters in the Lincolnshire Chalk is shown in Fig. 6.13; the end-point waters are a low chloride water and the local modern seawater. The diagram shows an enrichment in potassium with respect to chloride for many of the groundwaters, which is attributed to ion exchange occurring in the aquifer.

6.4.8. Mixing diagrams

While dilution diagrams represent a theoretical mixing between two waters, their main function is to indicate deviations from the theoretical condition. Where waters fall on a dilution line a possible mixing percentage can be calculated; similarly, as shown in Fig. 6.14 mixing percentages between three groundwaters can be calculated. Mixing based on two parameters, however, can lead to fallacious conclusions so that the process is better represented using the whole suite of major ions as depicted in Fig. 6.15. In this figure intercepts on the straight-line relationships between the end-point waters give the percentage of true

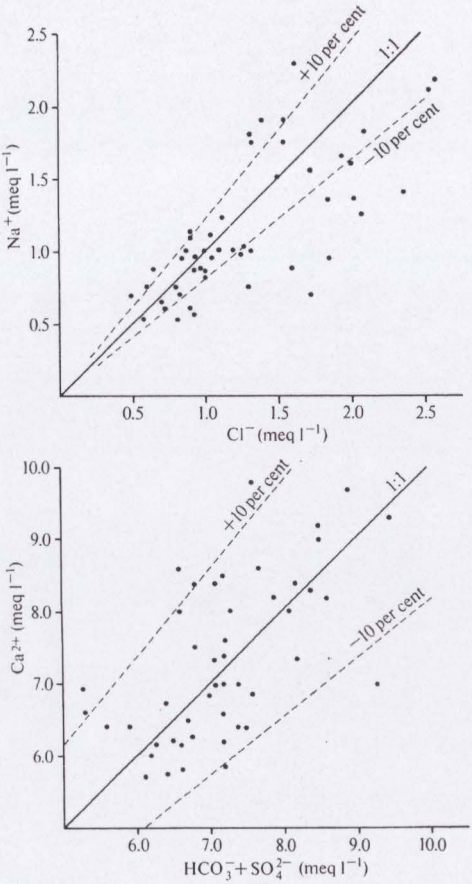

Fig. 6.12. *X–Y* plot of major ions showing simple dissolution.

mixing that has occurred. Deviations from a straight-line relationship indicate a complicating process occurring in addition to mixing.

Where actual mixing is found to occur between three waters multiparameter confirmation is difficult graphically although it has been attempted by McKinnell (1958).

6.4.9. Trilinear diagrams

The use of trilinear diagrams to represent groundwaters was first attempted by Hill (1940) and refined by Piper (1944). The Piper diagram has become universally used and is shown in Fig. 6.16. Major ions are plotted in the two base triangles of the diagram as cation and anion percentages of milliequivalents per litre. Total cations and total anions are each considered as 100 per cent. The

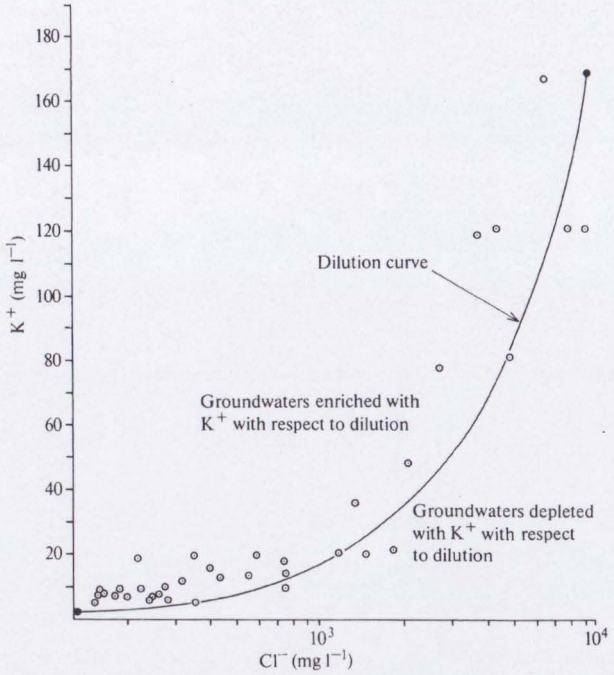

Fig. 6.13. Dilution diagram for a groundwater data set relating Cl^- and K^+: •, end-point waters.

respective cation and anion locations for an analysis are projected into the rectangle which represents the total ion relationships, as shown on Fig. 6.16.

The Piper diagram allows comparisons to be made between a large number of analyses but has the drawback that all trilinear diagrams have in not portraying actual ion concentrations. The distribution of ions within the main field rectangle is unsystematic in hydrochemical process terms so that the diagram lacks a certain logic. Further, the large amount of line work is a hindrance.

As shown on Fig. 6.16 total dissolved solids can also be represented on a Piper diagram by circles drawn at analysis locations in the rectangle. Circle radii as shown are normally proportional to logarithmic values of total dissolved solids.

The diagram can be used to calculate resultant mixing between two groundwaters if the groundwaters plot on a straight line in each of the three fields. To demonstrate conclusively that simple mixing is occurring Piper (1944) recommends that the graphical conclusion is substantiated by calculations.

An alternative diagram to that of Piper has been devised by Durov (1948) and is shown in Fig. 6.17. As with the former diagram it is normally based upon percentage major ion milliequivalent values, but in this case the cations and

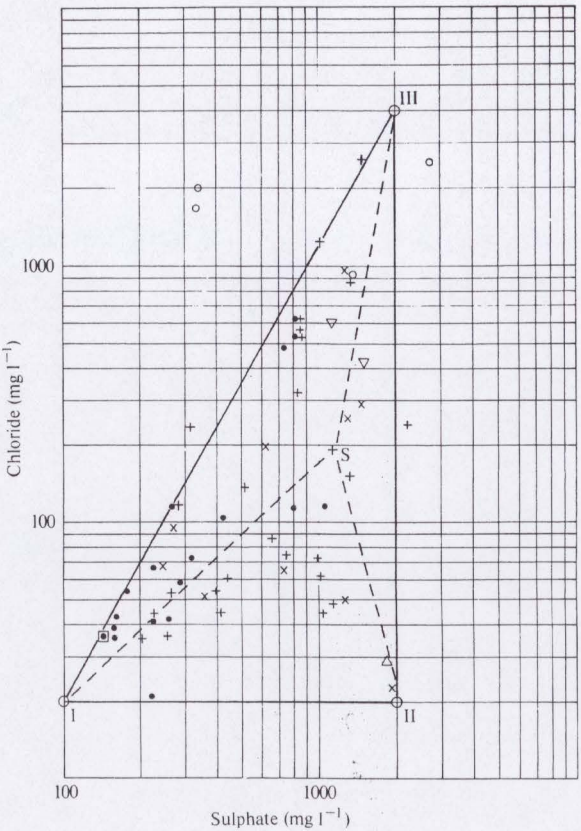

Fig. 6.14. Set of groundwaters representing mixing of the three end-point waters I, II, and III. The mixed water S is composed of 47.5%, I, 48.3% II, and 4.2% III.

anions together total 100 per cent. The cation and anion values are plotted in the appropriate triangle and projected into the square main field as shown on Fig. 6.17.

An expanded version of the Durov diagram is shown in Fig. 6.18. In this diagram, developed by Burdon and Mazloum (1958) and Lloyd (1965), the cation and anion triangles are recognized and are separated along the 25 per cent axes so that the main field is conveniently divided. On Fig. 6.17 the extension of the diagram to include a seventh parameter is shown. While total dissolved solids are shown in this case, clearly any parameter can be used.

The expanded Durov diagram has the distinct advantage over the Piper diagram in that it provides a better display of hydrochemical types and some processes, and in practical terms has less line work in the main field. Although,

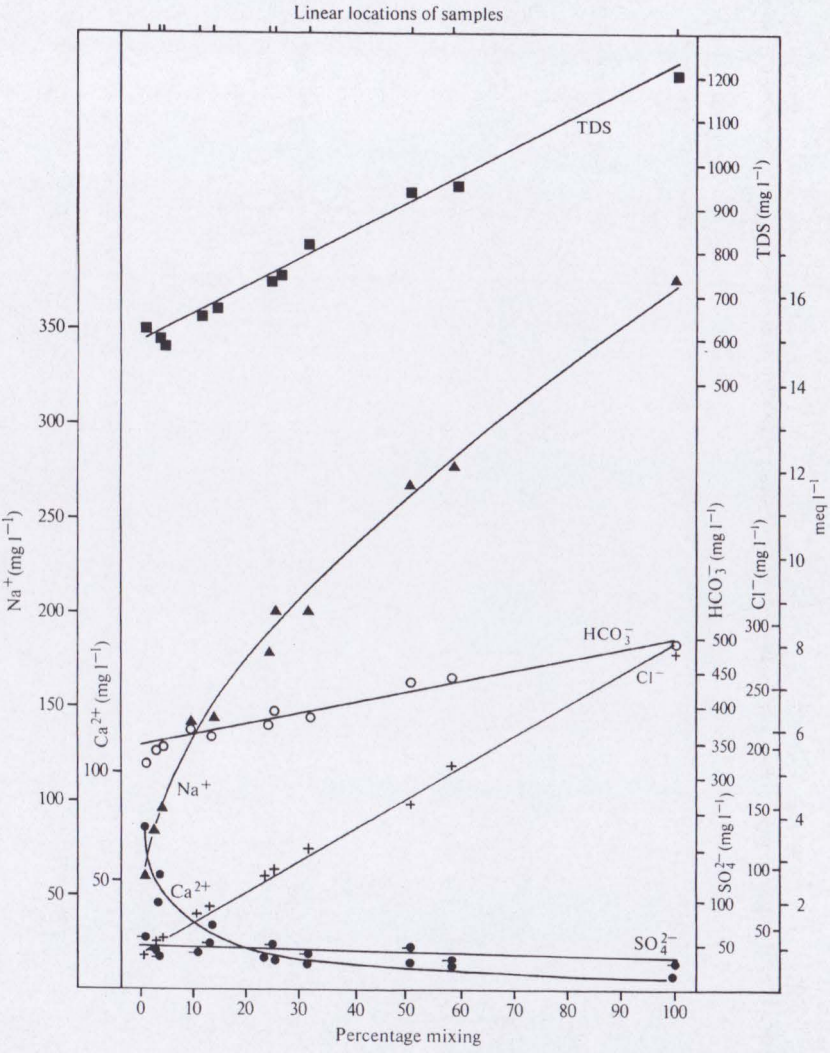

Fig. 6.15. Mixing diagram showing ion exchange. (After Lawrence *et al.* 1976.)

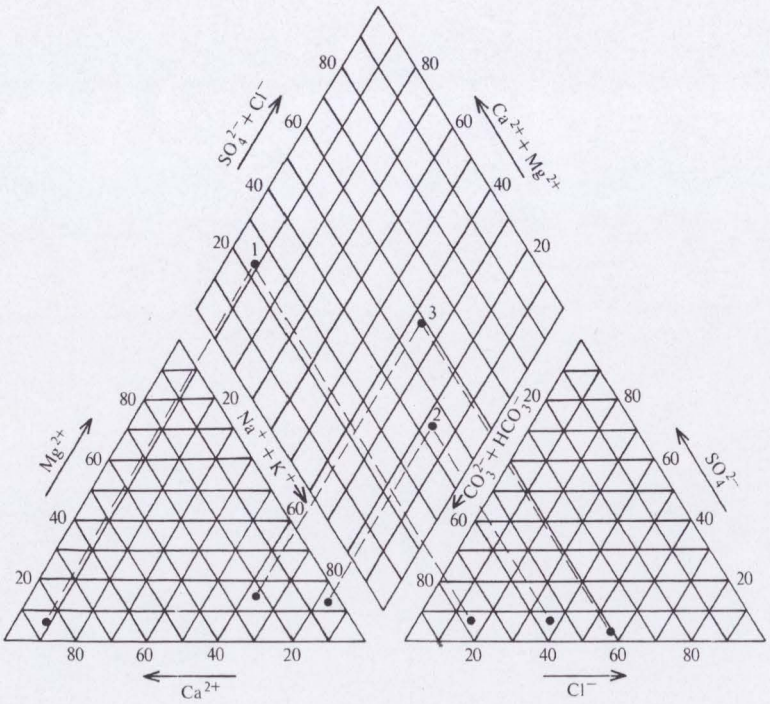

	1			2			3		
	mg l^{-1}	meq l^{-1}	Per cent	mg l^{-1}	meq l^{-1}	Per cent	mg l^{-1}	meq l^{-1}	Per cent
Ca^{2+}	152	7.58	85.5	8	0.40	4.0	85	4.24	22.3
Mg^{2+}	5.8	0.48	5.4	15.5	1.28	12.8	35	2.88	15.2
Na^+	17	0.74	8.3	186	8.09	81.4	270	11.74	61.8
K^+	2.8	0.07	0.8	7	0.18	1.8	6	0.15	2.8
HCO_3^-	404	6.61	77.7	326	5.34	55.8	479	7.84	40.6
SO_4^{2-}	29	0.60	7.1	37	0.77	8.0	29	0.60	3.1
Cl^-	46	1.30	15.2	123	3.47	36.2	286	10.89	56.3

Fig. 6.16. Trilinear diagram of major ions. (After Piper 1944.)

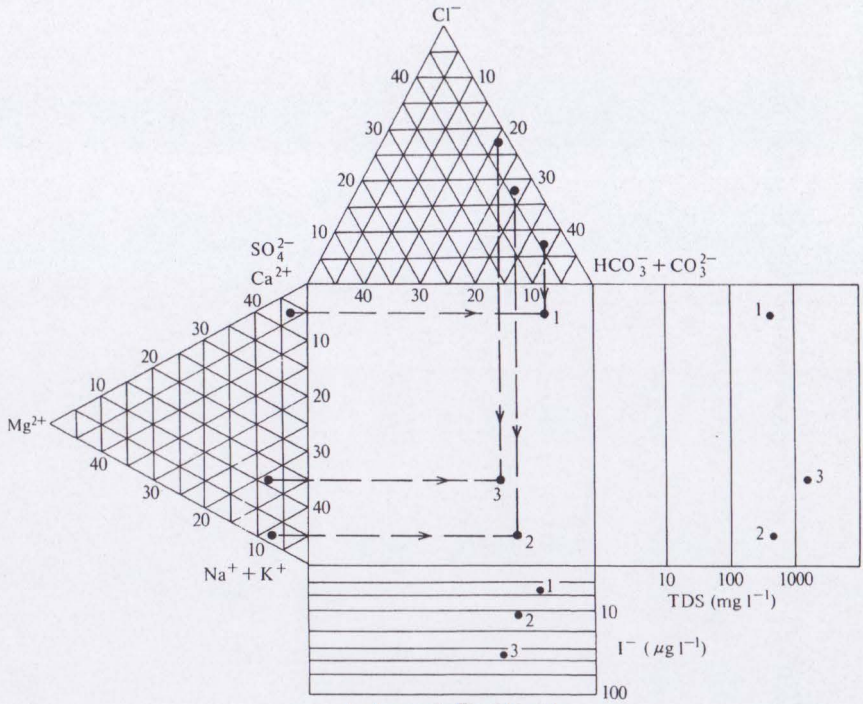

	I^-	TDS
1	2.7	660
2	10.4	710
3	3.4	1190

Fig. 6.17. The original type of Durov diagram.

as is shown on Fig. 6.18, waters with a 25 per cent concentration of a certain ion can theoretically plot ambiguously, in practice the ambiguity has little relevance and can be solved by the association of the problem water with neighbouring waters.

The significance of the nine fields on the expanded Durov diagram can be discussed with respect to Fig. 6.19 as follows:

1. HCO_3^- and Ca^{2+} dominant, frequently indicates recharging waters in limestone, sandstone, and many other aquifers.

2. HCO_3^- dominant and eight Mg^{2+} dominant or cations indiscriminant, with Mg^{2+} dominant or Ca^{2+} and Mg^{2+} important, indicates waters often associated with dolomites; where Ca^{2+} and Na^+ are important partial ion exchange may be indicated.

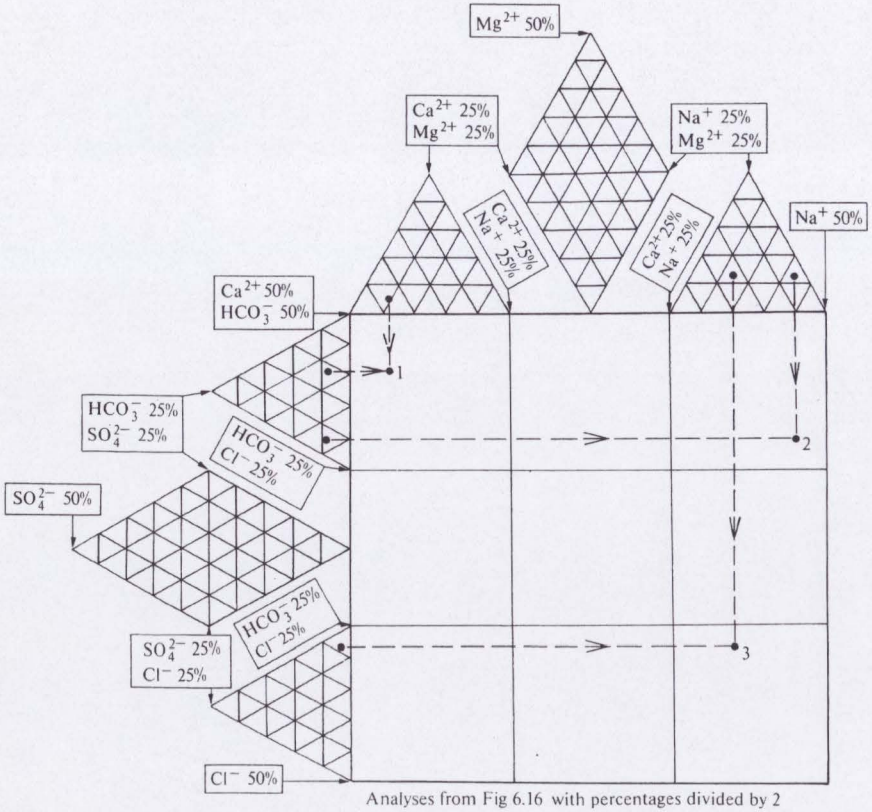

Fig. 6.18. Expanded Durov diagram demonstrating major ions.

3. HCO_3^- and Na^+ dominant, normally indicates ion-exchanged waters although the generation of CO_2 at depth can produce HCO_3^- where Na^+ is dominant under certain circumstances (Winograd and Farlekas 1974).

4. SO_4^{2-} dominant or anions indiscriminant and Ca^{2+} dominant, Ca^{2+} and SO_4^{2-} dominant frequently indicates a recharge water in lavas and gypsiferous deposits; otherwise a mixed water or a water exhibiting simple dissolution may be indicated (see Fig. 6.20).

5. No dominant anion or cation, indicates waters exhibiting simple dissolution or mixing.

6. SO_4^{2-} dominant or anions indiscriminant and Na dominant, is a water type not frequently encountered and indicates probable mixing influences.

7. Cl^- and Ca^{2+} dominant, is infrequently encountered unless cement pollution is present in a well; otherwise the waters may result from reverse ion exchange of $Na^+ - Cl^-$ waters.

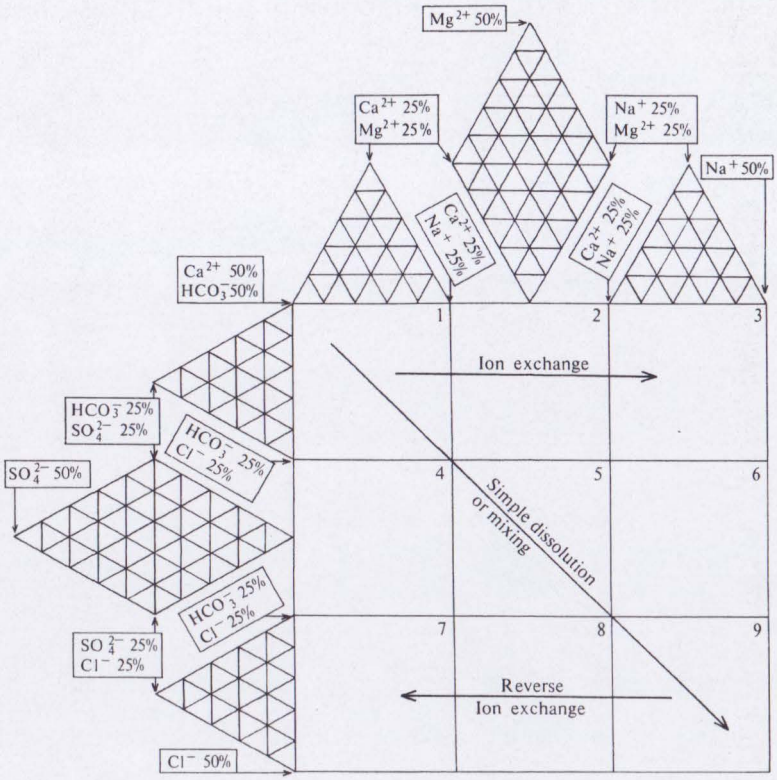

Fig. 6.19. Expanded Durov diagram with subdivisions and processes demonstrated.

8. Cl^- dominant and no dominant cation indicates that the groundwaters may be related to reverse ion exchange of Na^+-Cl^- waters.

9. Cl^- and Na^+ dominant frequently indicates end-point waters. The Durov diagram does not permit much distinction between Na^+-Cl^- waters.

The arrows in Fig. 6.19 indicate possible process paths such as ion exchange or dissolution. Care, however, has to be exercised as demonstrated in Fig. 6.20 in which a simple mixing between a recharge water and brackish water is shown to fall in five of the plotting fields.

By sensible interpretation of the expanded Durov diagram groundwaters can be classified or typed as shown on Fig. 6.21 using simple groupings. The same method can also be applied to parts of the Durov diagram if distinctive waters are present (Fig. 6.22).

Although the Durov diagram has been extensively applied to major ion

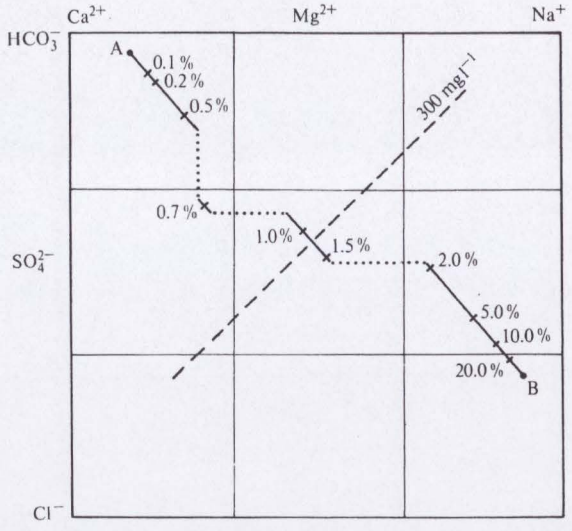

Fig. 6.20. Groundwater mixing demonstrated on the Durov diagram: curve A, fresh groundwater; curve B, brackish groundwater. (Percentage is mix between A and B.)

chemistry it can also be used to represent minor ions for groundwater typing purposes as shown on Fig. 6.23.

6.4.10. Statistical diagrams and techniques

Statistical diagrams are not extensively used in groundwater chemistry because the complexity of hydrochemical processes does not readily permit statistics to be realistically applied.

Hem (1970) discusses the use of cumulative percentage composition diagrams. Such diagrams have similar representation characteristics to Schoeller diagrams but are of very limited value.

Probability diagrams provide more information and can be used particularly in the early stages of interpretation to distinguish between waters. They are frequently favoured in isotope hydrochemistry and as shown in Fig. 6.24 changes in probability trend are considered to reflect differing ^{18}O groundwaters from Southern Arabia.

Multivariate analyses, although attempted, have been difficult to understand in relation to hydrochemical studies. Dalton and Upchurch (1978) have used principal component analysis, but generally the method provides little hydrochemical insight while Ashley and Lloyd (1978) have reviewed cluster and factor methods and applications, and found them to be of marginal value.

Superficially cluster and factor analyses would appear to offer more powerful methods of interpreting hydrochemical data than the conventional ones.

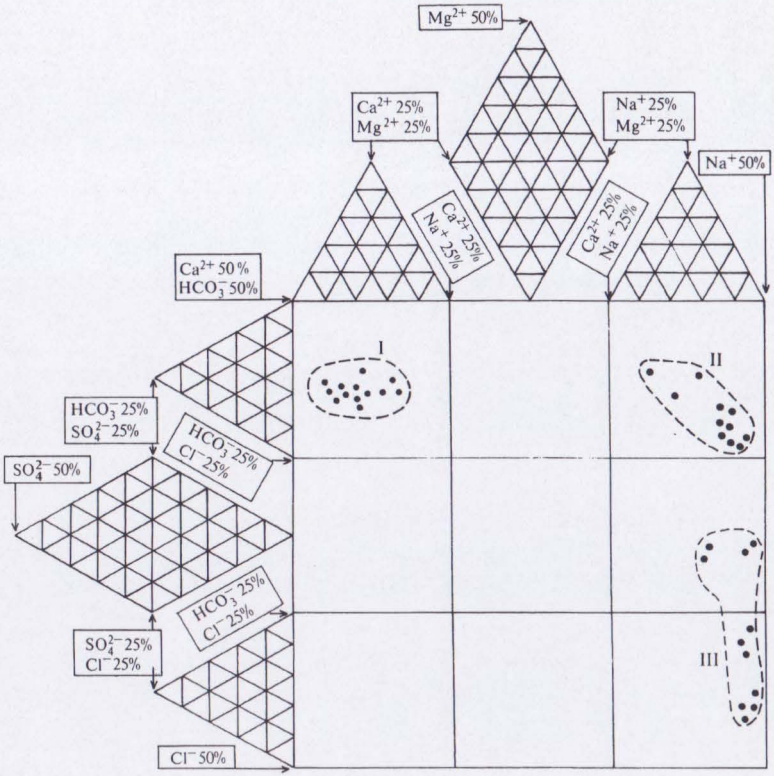

Fig. 6.21. Water types grouped using a Durov diagram: I, fresh recharge water; II, ion exchanged water; III, old brackish water.

Ashley and Lloyd (1978), however, have found that the statistical and conventional approaches usually provide the same results. Unfortunately cluster and factor analyses require considerable data handling with data normalization and can only be effective with good computer facilities. A cluster analysis output for groundwaters in the Gamogara area in Southern Africa is shown in Fig. 6.25 (Smith 1980); five groups of groundwaters are identified at or below a significance of 1.5 (Davis 1973) and are represented as a distribution on Fig. 6.26. While the distribution proved hydrogeologically significant in the study, the same grouping was more easily obtained using trilinear grouping methods. Further, many of the groundwaters could not be grouped using the dendrogram.

The approach of mapping statistical groupings has also been followed in factor analysis. The statistical method is outside of the scope of this book (see Davis 1973); however, the method resolves a set of multivariate factors in which

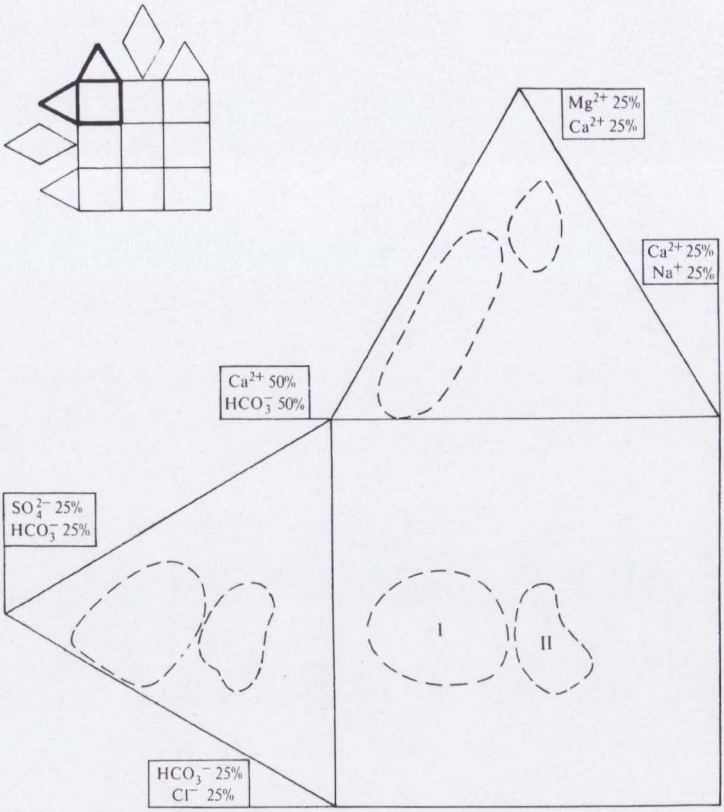

Fig. 6.22. Water-type grouping in a sector of a Durov diagram: I, Ca^{2+}-dominant recharge: II, Mg^{2+}-dominant recharge.

certain hydrochemical parameters may prove significant. The factors themselves, though statistically significant, have no hydrochemical significance, so if plotted on a distribution map their significance relates to the dominant hydrochemical parameter weighting the factor. A factor distribution from groundwaters in the alluvial Santiago Basin in Chile is shown in Fig. 6.27. The factor has a high silica weighting with the 'extreme' values related to:

(i) where the Mapocho River enters the basin after draining part of a granite intrusion further east;

(ii) down gradient of basement high areas where groundwater in the alluvium is moving slowly;

(iii) where runoff to the basin occurs from granitic intrusion along the northwestern and western margins of the basin.

The value of the factor analysis in this case was to draw attention to the significance of silica which otherwise may have been overlooked.

	mg l^{-1}	Per cent
F^-	210	28.3
Li^+	10	1.4
Sr^{2+}	150	20.3
I^-	5	8.1
B	15	24.2
Br^-	11	17.7

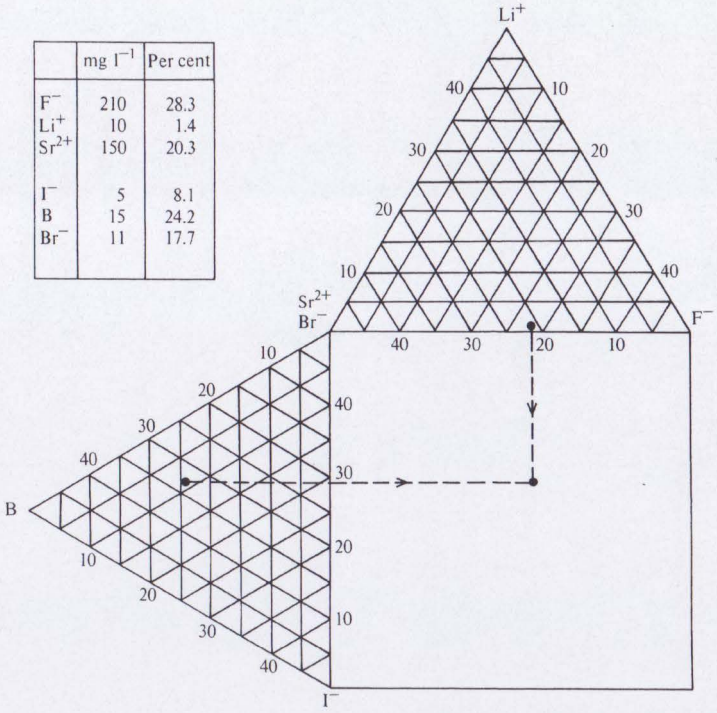

Fig. 6.23. Minor ion chemistry represented by a Durov diagram.

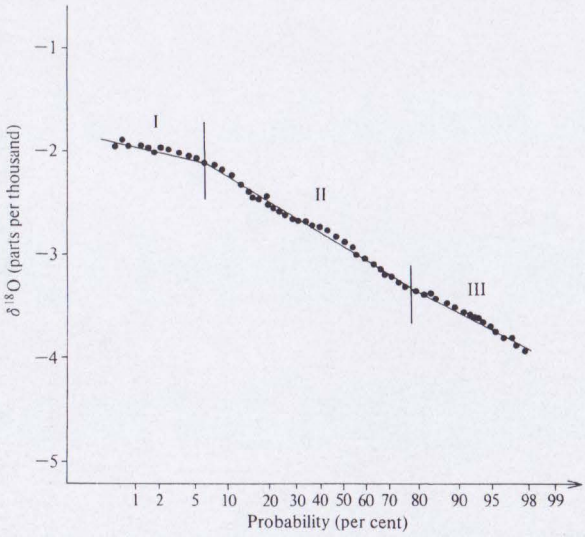

Fig. 6.24. Probability diagram used for grouping groundwaters: I–III, possible ^{18}O groupings based upon probability.

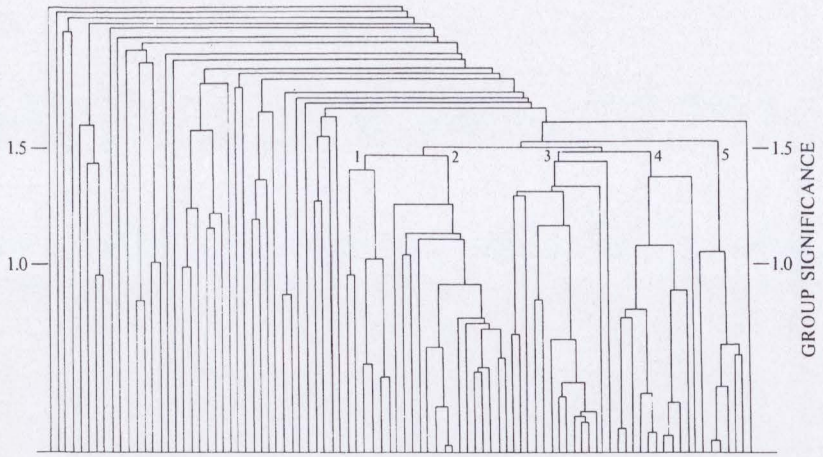

Fig. 6.25. Cluster dendrogram for groundwaters from Gamoşara in Southern Africa: 1–5, groups at a significance of 1.5. (After Smith 1980.)

Trend surface analyses are frequently used for determining parameter distribution in geology. An example of their application to groundwater chemistry is shown on Fig. 6.28 for the Murray Basin of Australia. Such analyses can provide an initial guide for interpretation but tend to produce unrealistic hydrochemical patterns owing to data distribution bias. One useful aspect of trend surface analysis is that differences between surfaces of different degrees can indicate areas of hydrochemical anomaly.

6.5. Conclusions

To represent groundwater chemistry a simple but effective approach which can easily be computerized can be adopted as follows:

(i) analyse data to provide initial X-Y plots which should allow recognition of variations in data relationships and indications of chemical processes and anomalies;

(ii) prepare distribution maps and hydrochemical sections of pertinent parameters;

(iii) in conjunction with (ii) distinguish water types or groupings using preferably a Durov-type plot;

(iv) represent any particular hydrochemical relationship on the most appropriate diagram (e.g. a dilution diagram).

While hydrochemical representation appears simple, it is very important in helping to interpret hydrochemical conditions and time spent in sensibly attaining a good representation can be very worthwhile.

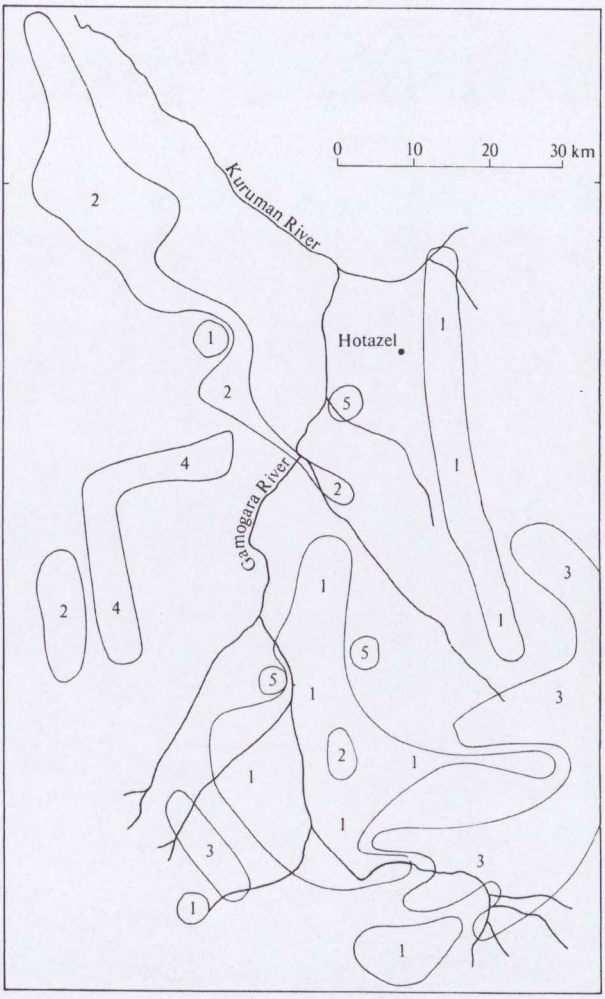

Fig. 6.26. Distribution of cluster dendrogram groups from Fig. 6.25. 1–5 relates to groups at a significance of 1.5 as shown in Fig. 6.25. Groundwaters lying outside these areas cannot be grouped on the dendrogram.

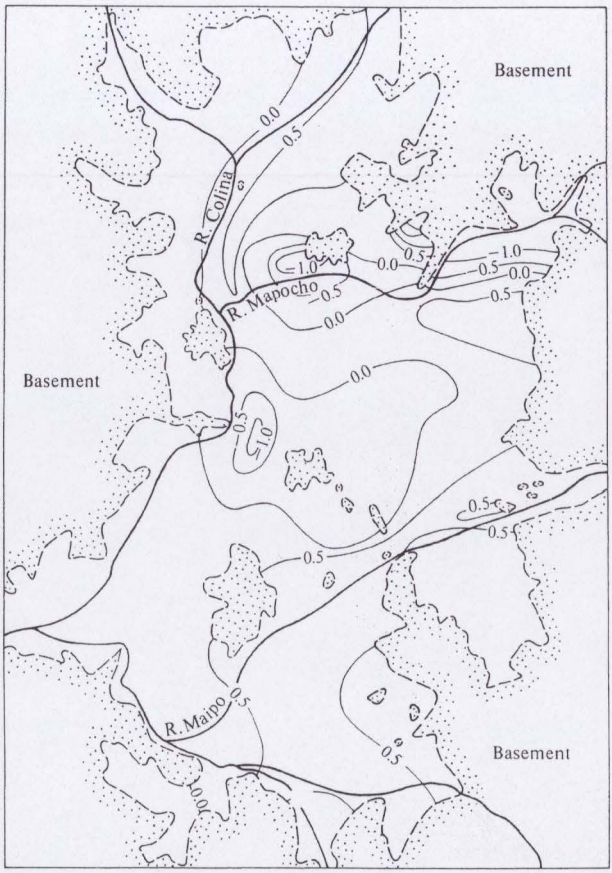

Fig. 6.27. Factor distribution for groundwaters in the alluvial aquifer of the Santiago Basin, Chile.

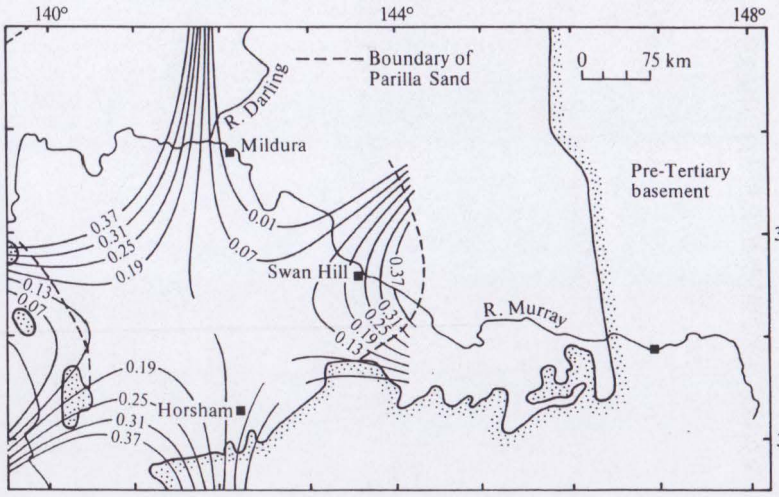

Fig. 6.28. Third degree surface map of HCO_3^-/Cl^- ratios of groundwater associated with the Parilla Sand, River Murray Basin, Australia. The percentage fit is 25.89%. (After Lawrence 1975.)

References

Ashley, R. P. and Lloyd, J. W. (1978). An examination of the use of factor analysis and cluster analysis in groundwater chemistry interpretation. *J. Hydrol.* **41**, 329–44.

Burdon, D. J. and Mazloum, S. (1958). Some chemical types of groundwater from Syria. *UNESCO Symp. Teheran*, pp. 73–90. Unesco, Paris.

Dalton, M. G. and Upchurch, S. G. (1978). Interpretation of hydrochemical facies by factor analysis. *Ground Water* **16**, 228–33.

Davis, J. C. (1973). *Statistics and data analysis in geology*. Wiley, New York.

Durov, S. A. (1948). Natural waters and graphic representation of their composition. *Dokl. Akad. Nauk SSSR* **59**, 87–90.

Hem, J. D. (1970). Study and interpretation of the chemical characteristics of natural water. *U.S. geol. Surv. water supply Pap. 1473.*

Hill, R. A. (1940). Geochemical patterns in the Coachella Valley, California. *Trans. Am. geophys. Union* **21**, 46–9.

Ineson, J. and Downing, R. A. (1963). Changes in the chemistry of ground waters of the Chalk passing beneath argillaceous strata. *Bull. geol. Surv. G.B.* **20**, 519–41.

Lawrence, A. R., Lloyd, J. W., and Marsh, J. M. (1976). Hydrochemistry and groundwater mixing in part of the Lincolnshire Limestone aquifer, England. *Ground Water* **14**, 12–20.

Lawrence, C. R. (1975). Geology, hydrodynamics and hydrochemistry of the southern Murray Basin. *Geol. Surv. Victoria, Mem. 30.*

Lloyd, J. W. (1965). The hydrochemistry of the aquifers of north-eastern Jordan. *J. Hydrol.* **3**, 319–30.

— (1969). The hydrogeology of the southern desert of Jordan. *UNDP/FAO. Pub. tech. Rep. 1. Special Fund 212.*

Marsh, J. M. (1977). Groundwater chemistry and its relation to flow in the southern Lincolnshire Limestone. *Univ. Birmingham Rep. Dept. Geol. Sci.*

Maucha, R. (1949). The graphical symbolisation of the chemical computation of natural waters. *Hydrol. Közölny* **13**, 117–18.

McKinnell, J. C. (1958), Indentification of mixtures of waters from chemical water analysis. *J. petrol. Technol. Tech. Note* **2016**, 79–82.

Piper, A. M. (1944). A graphic procedure in the geochemical interpretation of water analyses. *Trans. Am. geophys. Union*, 25, 914–23.

Schoeller, H. (1959). Arid zone hydrology—recent developments. *Arid Zone Research XII* UNESCO, Paris.

— (1962). *Les eaux souterraines.* Massio, Paris.

Smith, P. (1980). A re-assessment of the hydrogeological data from the Gamogora catchment, South Africa. *M. Sc. Project Rep., Dept. Geol. Sci. University of Birmingham.*

Stiff, H. A. (1951). The interpretation of chemical water analysis by means of patterns. *J. petrol. technol.* **3**, 15–17.

Winograd, I. J. and Farlekas, G. M. (1974). Problems in ^{14}C dating of waters from aquifers of deltaic origin. In *Isotope hydrology*, pp. 69–93. International Atomic Energy Agency, Vienna.